

**Titel/Title:**

**Autor\*innen/Author(s):**

Veröffentlichungsversion/Published version:

Publikationsform/Type of publication:

**Empfohlene Zitierung/Recommended citation:**

Verfügbar unter/Available at:

(wenn vorhanden, bitte den DOI angeben/please provide the DOI if available)

Zusätzliche Informationen/Additional information:

**Title:**

Grinding burn limits: Generation of surface layer modification charts for discontinuous profile grinding with analogy trials

**Authors:**

Nikolai Guba <sup>a) b)\*</sup>

Jonas Heinzl <sup>a) b)</sup>

Carsten Heinzl <sup>a) b)</sup>

Bernhard Karpuschewski <sup>a) b)</sup>

a) Leibniz Institute for Materials Engineering, Division Manufacturing Technologies, Badgasteiner Straße 3, 28359 Bremen, Germany

b) University of Bremen and MAPEX Center for Materials and Processes, Bibliothekstr. 1, 28359 Bremen, Germany

\*Corresponding author at: Leibniz Institute for Materials Engineering, Division Manufacturing Technologies, Badgasteiner Straße 3, 28359 Bremen, Germany

E-mail address: [guba@iwt-bremen.de](mailto:guba@iwt-bremen.de)

**Abstract:**

By means of surface layer modification charts, the occurrence of thermal impact and thus the risk of grinding burn can be detected. With the present work it was shown that surface layer modification charts for discontinuous profile grinding can be generated using analogy trials carried out on a surface grinding machine for investigation of different grinding conditions and varied tilt angles in profile grinding. The experimental and the analysis effort for the analogy trials prove to be significantly more time and cost saving. The results also suggest that system parameters such as the grinding wheel specification or the cooling strategy are taken into account by the specific grinding power. Thus, the experimental results of this work allow the assumption that the determined process limit is not or just to a low extent depending on the system parameters. This assumption is supported by the thermal process limit determined by Malkin and converted in surface layer modification charts. Malkin's limit, identified for different ground steels with surface and cylindrical grinding processes and thus different system and process parameters, corresponds to the results generated in this work at workpieces ground with a kinematically more complex process. The results reveal that there is at least a group of steel materials which **seems to share a similar thermal** process limit.

**Keywords:**

Gear profile grinding, thermal process limit, analogy trial, analytic process model

## Nomenclature

Abbreviations	Unit	Designation
$a_e$	$\mu\text{m}$	depth of cut
$a_{ed}$	$\mu\text{m}$	dressing depth of cut
$a_p$	mm	width of cut
$B$	$\text{J}/(\text{mm}^2 \text{s}^{0.5})$	factor (Malkin)
$b$	mm	toothed width
$d$	mm	pitch diameter
$d_{eq}$	mm	equivalent wheel diameter
$d_s$	mm	grinding wheel diameter
$d_{s,eff}$	mm	effective grinding wheel diameter
$e_c$	$\text{J}/\text{mm}^3$	specific grinding energy
$e_c^*$	$\text{J}/\text{mm}^3$	critical specific grinding energy
$e_w$	$\text{J}/\text{mm}^3$	basis value of the specific grinding energy
$F_n$	N	normal force
$F_p$	$\mu\text{m}$	Pitch deviation
$F_t$	N	tangential force
$F_t''$	$\text{N}/\text{mm}^2$	specific tangential force
$F_r$	$\mu\text{m}$	concentricity deviation
$F_\alpha$	$\mu\text{m}$	total profile deviation
$F_\beta$	$\mu\text{m}$	total flank deviation
$H$	mm	height
$K_0$	-	modified Bessel function
$k$	$\text{W}/(\text{m}\cdot\text{K})$	thermal conductivity
$L$	mm	length
$L$	-	dimensionless half length of the heat source
$l$	mm	half-length of source
$l_g$	mm	contact length
$m_n$	mm	normal module
mp-value	mV	magnetoelastic parameter
$P_c$	W	grinding power
$P_c''$	$\text{W}/\text{mm}^2$	specific grinding power
$p$	-	Jaeger non-dimensional variable where $X-L \leq p \leq X+L$
$Q_{MWF}$	l/min	metal working fluid flow rate
$Q_w$	$\text{mm}^3/\text{s}$	material removal rate
$Q'_w$	$\text{mm}^3/(\text{mm}\cdot\text{s})$	specific material removal rate
$q_d$	-	dressing speed ratio
$q_w$	$\text{W}/\text{mm}^2$	heat flux density
$T$	$^\circ\text{C}$	temperature
$T_{max}$	$^\circ\text{C}$	maximum contact zone temperature
$t$	s	time
$U_d$	-	overlapping ratio
$v_c$	m/s	cutting speed
$v_d$	m/s	dressing speed
$v_f$	mm/min	feed speed
$v_{fa}$	mm/min	axial feed speed
$v_{ft}, v_w$	mm/min	tangential feed speed
$W$	mm	width
$W_k$	mm	span
$X$	-	dimensionless distance to the center of heat source
$x$	mm	coordinate in direction of $v_{ft}$
$x_0$	mm	displacement in direction of $x$
$x \cdot m_n$	mm	addendum modification
$Z$	-	dimensionless depth beneath the work-piece surface

$z$	-	number of teeth
$z$	mm	depth beneath the workpiece surface
$\alpha$	mm <sup>2</sup> /s	thermal diffusivity
$\alpha_n$	°	normal pressure angle
$\beta$	°	helix angle
$\Delta s$	μm	material stock to be removed
$\Delta s_1$	μm	material stock to be removed at the beginning of the grinding process
$\Delta s_2$	μm	material stock to be removed at the end of the grinding process
$\Delta t$	s	contact time
$\varepsilon$	-	grinding energy partition
$\lambda$	W/(m·K)	thermal conductivity
$\varphi$	°	tilt angle

## 1. Introduction and state of the art

The determination of critical process limits of the grinding process is of particular importance in order to achieve a productive process design in manufacturing workpieces [1]. Exceeding the thermal process limit of the grinding process can cause the occurrence of tensile residual stresses, tempered or rehardened zones within the surface layer of the ground workpiece steel material [2, 3]. These negative surface layer properties have an essential impact on the functional properties such as fatigue strength and wear resistance of the ground workpieces [4]. The occurrence of tempered or rehardened zones as well as tensile residual stresses can lead to a significant reduction in wear resistance and fatigue strength and thus to a reject of the machined workpieces [5, 6]. In-process measurement technology for the determination of process quantities (process forces  $F$  or grinding power  $P_c$ ) and analytical process models based on them can be used to identify thermal process limits during grinding. In grinding technology, corresponding process models with reference to thermally induced surface and sub-surface layer influence are often attributed to the moving heat source according to Carslaw and Jaeger [7, 8, 9]. The heat conduction differential equation of the moving heat source (equation 1) can be solved by an approximated solution, a two-dimensional temperature field (equation 2). Taking into account grinding parameters referring to the surface layer ( $Z=0$  in equation 2) Malkin was able to establish a grinding burn limit for the processing of hardened steels more than 40 years ago [10].

$$\nabla^2 T = \frac{1}{\alpha} \left[ \frac{\partial T}{\partial t} - v_{ft} \frac{\partial T}{\partial x} \right] \quad (1)$$

$$T(X, Z) = \frac{2\alpha \cdot q_w}{\pi \cdot \lambda \cdot v_{ft}} \cdot \int_{X-L}^{X+L} e^{-p} \cdot K_0 \sqrt{p^2 + Z^2} \cdot dp \quad (2)$$

with the modified Bessel function  $K_0$ , the dimensionless parameters

$$X = \frac{v_{ft} \cdot X}{2 \cdot \alpha}, Z = \frac{v_{ft} \cdot Z}{2 \cdot \alpha}, L = \frac{v_{ft} \cdot l_g}{2 \cdot \alpha} \text{ and } p = \frac{v_{ft} \cdot (X - X_0)}{2 \cdot \alpha} \text{ according to [11].}$$

Based on the assumption that a critical temperature at the surface is necessary to produce grinding burn, which can be determined by nital etching, Malkin empirically determined a linear relationship between the specific grinding energy  $e_c^*$  (equation 3) and a product of process and system parameters at which grinding burn occurs [10, 12].

$$e_c^* = e_w + B \cdot d_{eq}^{0.25} \cdot a_e^{-0.75} \cdot v_w^{-0.5} = \frac{P_c}{Q_w} \quad (3)$$

The limit represents an isotherm, so that according to Malkin, the maximum temperature becomes comparable to the eutectoid temperature of steel of 723°C [12], which must be applied at least to the workpiece surface in order to generate grinding burn.

The factor B describes the slope of specific grinding energy if it is plotted versus the product  $d_{eq}^{0.25} \cdot a_e^{-0.75} \cdot v_w^{-0.5}$  [12, 13]. When applying Malkin's approach, it must be taken into account that a semi-infinite body and a constant energy  $e_w$ , which is generated in the process and which does not go into the workpiece, is assumed. Malkin was able to reveal the relationship described in equation 3 in surface and cylindrical grinding processes of hardened steels whereby conventional wheels and different cooling conditions (wet and dry) were used. Process and system parameters of his trials are presented in detail in [10].

In kinematically more complex grinding processes such as discontinuous profile grinding of case hardened gears, an increased risk of grinding burn due to line contact between grinding wheel and workpiece can occur [14]. In industry the discontinuous profile grinding process is used for hard fine machining of gears with module sizes  $m$  up to 40 mm [15]. To avoid grinding burn, especially when machining small batch sizes, often very small depths of cut are chosen, which in turn has a negative effect on the productivity. Currently, there are several approaches to avoid workpiece thermal damage during grinding. These approaches are based on critical values of process parameters, such as the depth of cut or the tangential feed speed which were identified by grinding experiments [16, 17, 18]. In order to detect grinding burn quickly and avoid it by adjusting the process parameters systematically, the approach of surface layer modification charts was developed (Figure 1, type 1) [19].

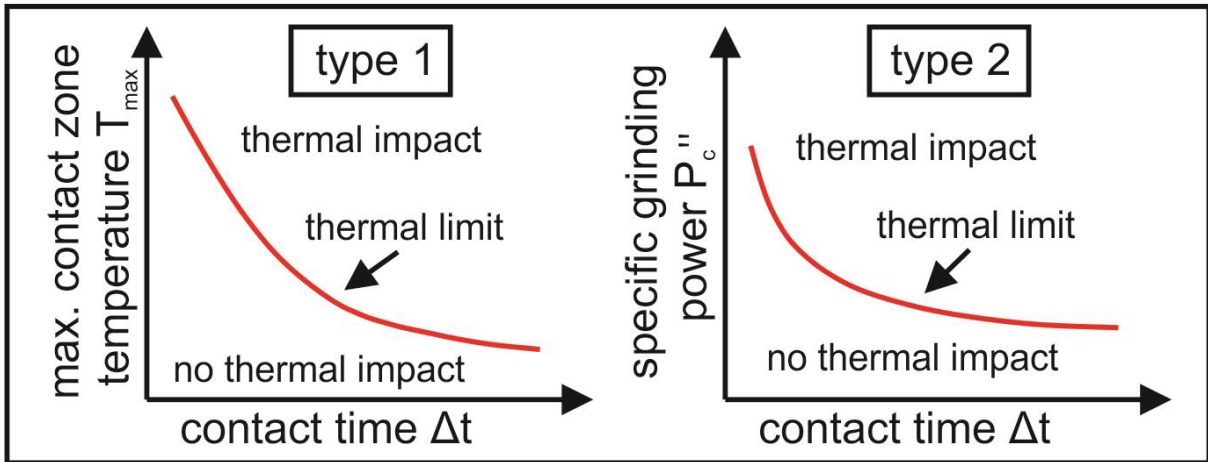


Figure 1. Two types of surface layer modification charts considering either the max. contact zone temperature or the specific grinding power.

In surface layer modification charts, the maximum contact zone temperature  $T_{\max}$  is plotted against the contact time  $\Delta t$ . The contact time can be calculated using equation 4.

$$\Delta t = \frac{l_g}{v_f} = \frac{\sqrt{a_e \cdot d_{s,eff}}}{v_f} \quad (4)$$

The contact time is the quotient of the contact length  $l_g$  and the feed speed  $v_f$ , whereby the depth of cut  $a_e$  and the effective grinding wheel diameter  $d_{s,eff}$  are required to calculate the contact length. The contact time corresponds to the duration that one point on the machined surface is within the contact zone and is thus exposed to the heat generated in the contact zone. According to the idea to interpret the grinding process as a moving heat source the temperature  $T_{\max}$  describes a measure for the heat intensity and the contact time  $\Delta t$  a measure for its duration. In order to simplify the complex transient heat flow conditions during the process described by thermal analytical [20] and numerical model-based simulations [21, 22], it is assumed that a maximum temperature rise is present at the contact zone during the contact time. With diagrams of this kind, the possibility of a quick assessment whether or not grinding burn has occurred without the additional use of further analysis methods such as Barkhausen noise or nital etching is given. This allows a correction of the process parameters (depth of cut and feed speed) and prevents grinding burn. Furthermore, process limits can be identified and thus the productivity of the grinding process can be increased. The applicability of surface modification charts has already been proven for surface

1 and external cylindrical grinding of simple geometries [3, 23]. In [24] it was investigated  
2 whether surface layer modification charts can also be used for discontinuous profile  
3 grinding of gears and thus for complex geometries. For this investigation, a grinding  
4 wheel with an integrated temperature measuring system was used [25]. During grind-  
5 ing the maximum contact zone temperature at the pitch diameter of the gears was  
6 determined. Although the applicability of these diagrams could be shown for discontin-  
7 uous profile grinding of gears, especially two difficulties have been encountered.

- 8 • Grinding wheels with an integrated temperature measuring system are required for  
9 the measurement of the maximum contact zone temperature [25]. The use of sur-  
10 face layer modification charts (type1, Figure 1) is only possible in conjunction with  
11 such a grinding wheel since otherwise the maximum contact zone temperature dur-  
12 ing discontinuous profile grinding of gears could not be determined.
- 13 • For the generation of surface layer modification charts, a large number of gears  
14 must be ground in order to obtain sufficient data points in the area of thermal impact  
15 and in the area without thermal impact so that the thermal limit can be identified.  
16 After the grinding tests, the ground gears must be checked for grinding burn. Since  
17 individual teeth have to be eroded out for metallographic analysis, this is particularly  
18 time-consuming and cost-intensive compared to workpieces with simple geometry.

19 The following section shows how these two difficulties can be overcome.

## 20 2. Concept to describe burning limits in discontinuous gear profile grinding

### 21 *Consideration of heat intensity in discontinuous gear profile grinding by using 22 the grinding power $P_c$*

23 In order to enable the use of the surface layer modification charts independently from  
24 a temperature measurement system, they can be modified. The maximum contact  
25 zone temperature is replaced by the in-process measured process quantity specific  
26 grinding power  $P_c$  (Figure 1, type 2) [13]. Thus, the heat intensity of the moving heat  
27 source is expressed by a less complex and more industry-oriented measured value.  
28 According to equation 5, the specific grinding power is the quotient of the grinding  
29 power  $P_c$  and the width of cut  $a_p$  as well as the contact length  $l_g$ . Since the grinding  
30 power can be taken directly from the grinding machine and the width of cut as well as



the contact length are known, the calculation of the specific grinding power can be done without any further effort.

$$P_c'' = \frac{P_c}{a_p \cdot l_g} \quad (5)$$

A further advantage of using  $P_c''$  instead of  $T_{max}$  is, that there is a comparability of surface modification charts and Malkin's grinding limit approach. Due to the fact that both the surface layer modification charts and Malkin's model contributed valid results for the determination of thermal process limits in the past, Malkin's grinding process limit determined for different hardened steels together with the process limits determined in this work will be considered in new  $P_c''$ - $\Delta t$  diagrams for discontinuous profile grinding of gears. Malkin's grinding data have already been converted to  $P_c''$ - $\Delta t$  diagrams in [13] and are shown in Figure 2. The green dotted line represents a trendline and its function is revealed.

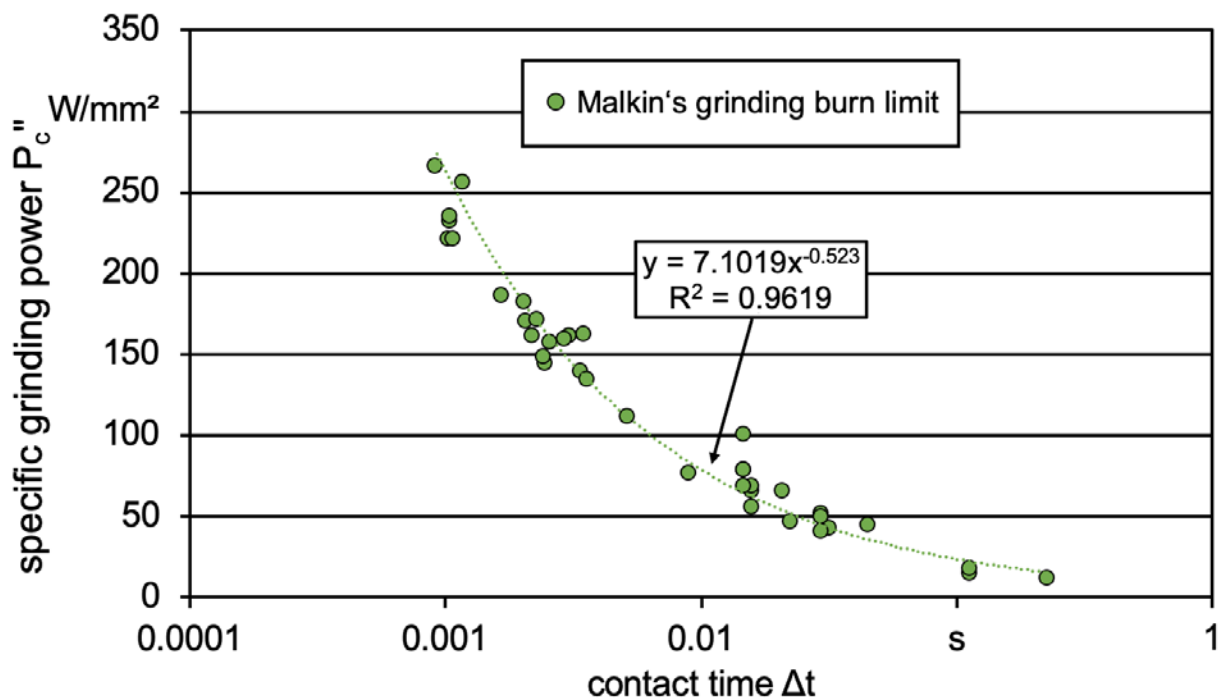


Figure 2. Experimental data from Malkin [10,13] in a surface layer modification chart (type 2,  $P_c''$ - $\Delta t$ ).

In [13], these data which based on Malkin's grinding burn limit for hardened steel were compared with experimental data from grind-hardening tests in surface and cylindrical



1 grinding. In grind-hardening, the process parameters of the grinding process intention-  
2 ally introduce so much heat into a non-heat-treated soft steel that final process step of  
3 grinding simultaneously leads to a martensitic hardening of the steel material [26], thus  
4 replacing the material heat treatment in the process chain [27, 28]. It could be shown  
5 that in tests with different workpiece material/grinding wheel/metal working fluid com-  
6 bination an area in  $P_c''-\Delta t$  diagrams can be identified in which a good grinding harden-  
7 ing result was achieved. This was evaluated on the basis of the hardness achieved  
8 and the hardening depth. This area lies above the process limit determined by Malkin  
9 for grinding of hardened steels, which seems to be plausible due to the influenced  
10 depth of material of grind-hardening compared to the first occurrence of grinding burn  
11 in Malkin's investigations. In spite of the fact, that the grind-hardening trials are not the  
12 focus of this work, the results lead to important conclusions. In particular the uniform  
13 area of successful grind-hardening tests, despite different system and process param-  
14 eters, raises the question of the dependency of a critical grinding process limit of hard-  
15 ened steels on these parameters. As already discussed in [13], the  $\xi$ -value, the pro-  
16 portion of energy which is converted into heat and goes into the workpiece may differ  
17 largely according to the actual grinding parameters and cooling conditions [28, 29, 30,  
18 31]. This difference is underlined by research works [27, 32, 33, 34], where different  
19 process parameters and cooling conditions led to different  $\xi$ -values. However, the  
20 methods for determining these values also differed.

### 21 ***Method for a time and cost saving generation of surface layer modification*** 22 ***charts with analogy trials***

23 In order to use simple geometries instead of gears for the generation of surface layer  
24 modification charts for discontinuous profile grinding, the analogy trials developed by  
25 Schlattmeier can be used [35]. According to Schlattmeier, every point along the invo-  
26 lute as well as the tooth root can be described using the tilt angle  $\phi$ . As shown in Figure  
27 3, the tilt angle results between the vertical line which is parallel to the centerline and  
28 the tangent at the considered point of the involute or the tooth root.

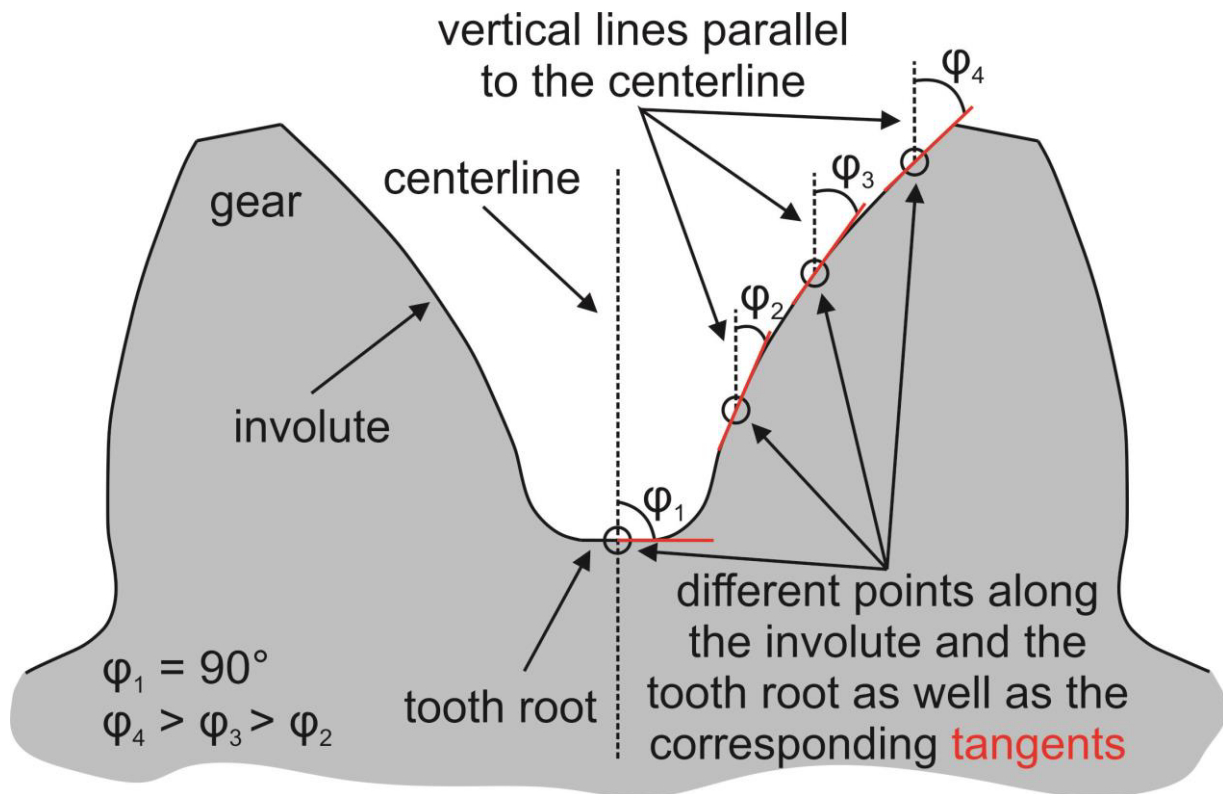


Figure 3. Tilt angle  $\varphi$  of different points along the gear tooth flank profile.

By using workpieces with corresponding tilt angles, the machining conditions for individual points along the involute as well as for the tooth root can be investigated. This also makes it possible to assess in which areas along the involute grinding burn is more likely to occur.

In the present work it was examined whether it is possible to generate surface layer modifications charts for discontinuous profile grinding of gears by means of analogy trials according to Schlattmeier. For this purpose, surface layer modifications charts type 2 were generated for discontinuous profile grinding and for grinding of workpieces with three different tilt angles (analogy trials). Then, both diagrams were combined, compared, and the alternative method for a time and cost saving generation of surface layer modification charts was assessed. In addition, an evaluation of the process limits for AISI 5120 (20MnCr5) determined by the surface layer modification charts was carried out on the basis of the grinding data determined by Malkin and transferred to a  $P_c$ "- $\Delta t$  diagram. In particular, the question of the dependency of the thermal process limits on process and system parameters of the grinding process was investigated.

### 3. Experimental setup and procedure

For the experiments gears and workpieces with three different tilt angles  $\varphi$  consisting of the case hardened steel AISI 5120 (20MnCr5) were used. Before grinding, the gears as well as the workpieces were conventionally case hardened. After the heat treatment the gears as well as the workpieces had a surface hardness of about 750 HV and a case hardening depth of approximately 1 mm. In Figure 4 the gear geometry and in Table 1 the gear parameters can be found.

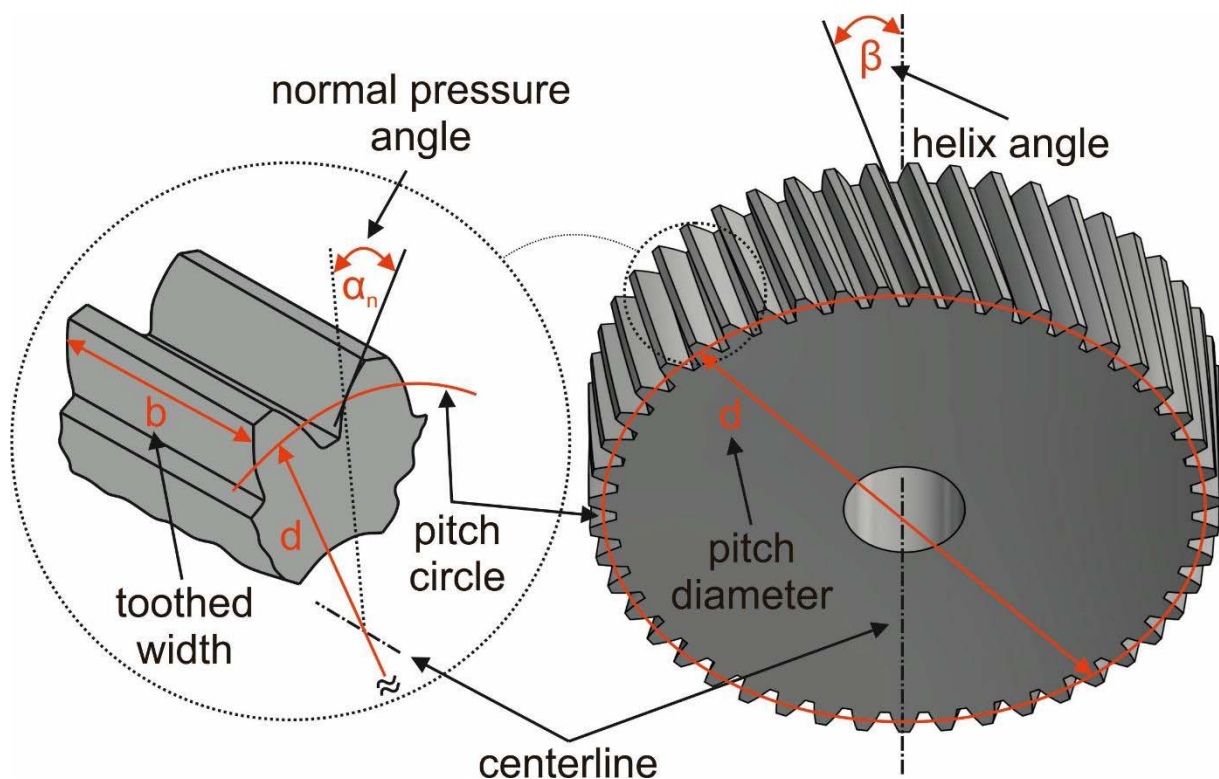


Figure 4. Geometry of the used gears for discontinuous profile grinding.

The experiments by discontinuous profile grinding were carried out on the gear grinding machine KX 500 Flex (Kapp GmbH & Co. KG). Gradually the specific material removal rate  $Q'_w$  was increased from  $22.5 \text{ mm}^3/(\text{mm}\cdot\text{s})$  in 2.5 steps to  $40 \text{ mm}^3/(\text{mm}\cdot\text{s})$ . At a constant specific material removal rate, seven different combinations of the radial depth of cut  $a_e$  and the axial feed speed  $v_{fa}$  were examined, whereby the axial feed speed was reduced starting at  $10000 \text{ mm/min}$  with increasing radial depth of cut. Using this procedure a total of 56 experiments were carried out, whereby each test was performed three times for statistical verification. At each experiment the grinding power

was measured with a sensor integrated directly on the grinding spindle. In order to ensure a uniform material removal according to the radial depth of cut and to compensate the distortion due to the heat treatment, the gears were pre-ground. After pre-grinding, the gears were measured geometrically (total flank deviation  $F_{\beta}$ , total profile deviation  $F_{\alpha}$ , concentricity deviation  $F_r$ , pitch deviation  $F_p$ , span  $W_k$ ) on the precision measuring center P40 (Klingelnberg GmbH) to ensure a comparable geometry and thus a common base for the main investigations. Table 1 summarizes the used grinding-, pre-grinding- and the dressing parameters as well as the grinding wheel specification and the cooling strategy.

Workpiece		Grinding parameters (Up grinding)	
Normal modul	$m_n = 4.5 \text{ mm}$	Cutting speed	$v_c = 35 \text{ m/s}$
Number of teeth	$z = 47$	Depth of cut	$a_e = 130 - 530 \text{ }\mu\text{m}$
Pitch diameter	$d = 220.66 \text{ mm}$	Width of cut	$a_p = 13.6 \text{ mm}$
Normal pressure angle	$\alpha_n = 24^\circ$	Axial feed speed	$v_{fa} = 2361 - 10000 \text{ mm/min}$
Helix angle	$\beta = 16^\circ 34'$	Specific material removal rate	$Q'_w = 22.5 - 40 \text{ mm}^3/(\text{mm}\cdot\text{s})$
Addendum modification	$x \cdot m_n = 2.222 \text{ mm}$	<b>Pre-Grinding parameters (Up grinding)</b>	
Toothed width	$b = 65 \text{ mm}$	Cutting speed	$v_c = 35 \text{ m/s}$
<b>Grinding wheel</b>		Depth of cut	$a_e = 5 \times 25 \text{ }\mu\text{m}$
Specification: 93A30F15VPH601W (sintered corundum + white corundum)		Axial feed speed	$v_{fa} = 3500 \text{ mm/min}$
Effective grinding wheel diameter $d_{s,eff} = 215.3 \text{ mm}$		<b>Dressing conditions</b>	
<b>Metal working fluid (MWF) supply</b>		Dresser: Electroplated diamond dressing roll form dressing (point contact)	
Oil-based (Houghton Cut-Max 902-10)		Dressing speed	$v_d = 35 \text{ m/s}$
Conventional tangential nozzle		Dressing depth of cut	$a_{de} = 2 \times 50 \text{ }\mu\text{m}$
Flow rate	$Q_{MWF} = 300 \text{ l/min}$	Overlapping ratio	$U_d = 4$
		Dressing speed ratio	$q_d = 0.7$

Table 1. Summary of the grinding, pre-grinding and dressing parameters as well as the gear parameters, the grinding wheel specification and the cooling strategy.

For the analogy trials, workpieces with tilt angles  $\varphi$  of  $90^\circ$ ,  $10^\circ$  and  $30^\circ$  were used. According to Figure 5, these workpieces can be used to investigate the machining conditions at the tooth root, the tooth flank and the tooth tip.

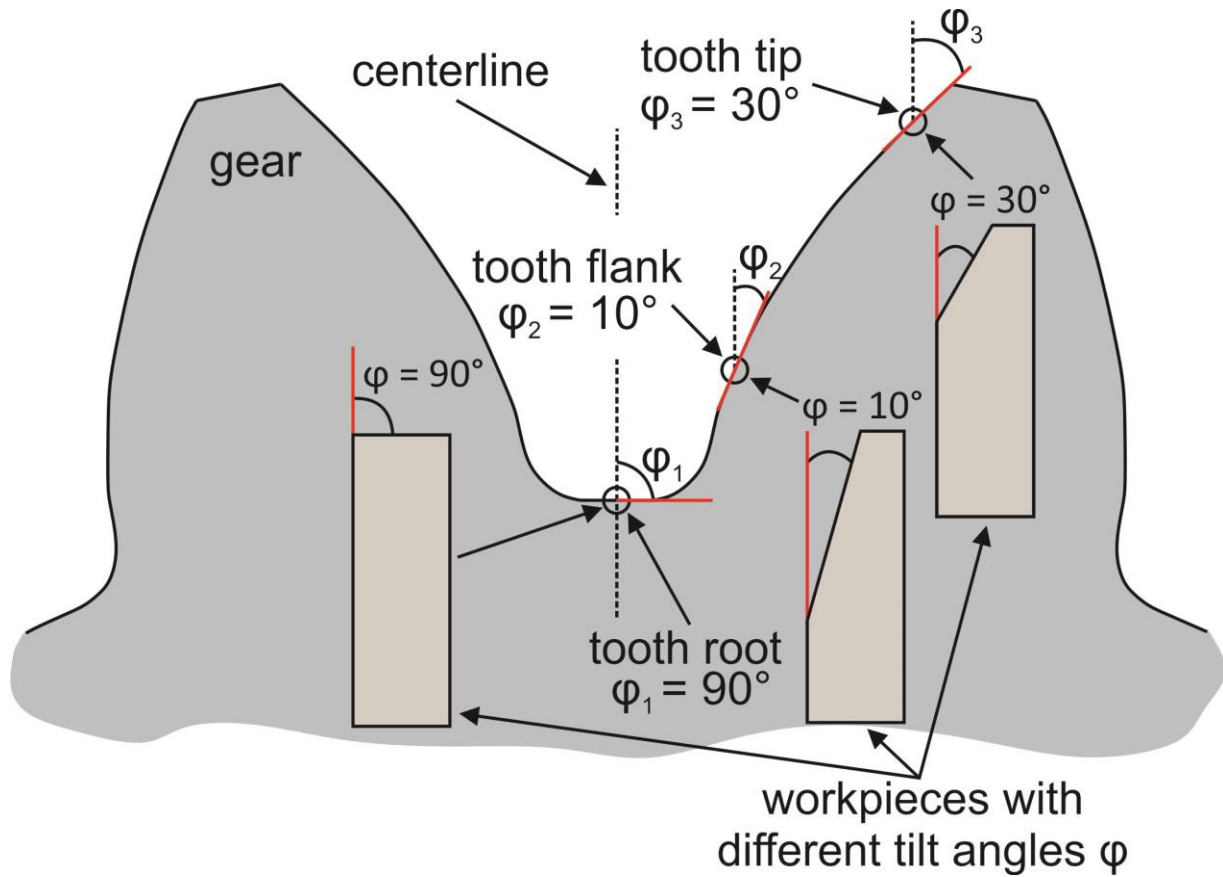
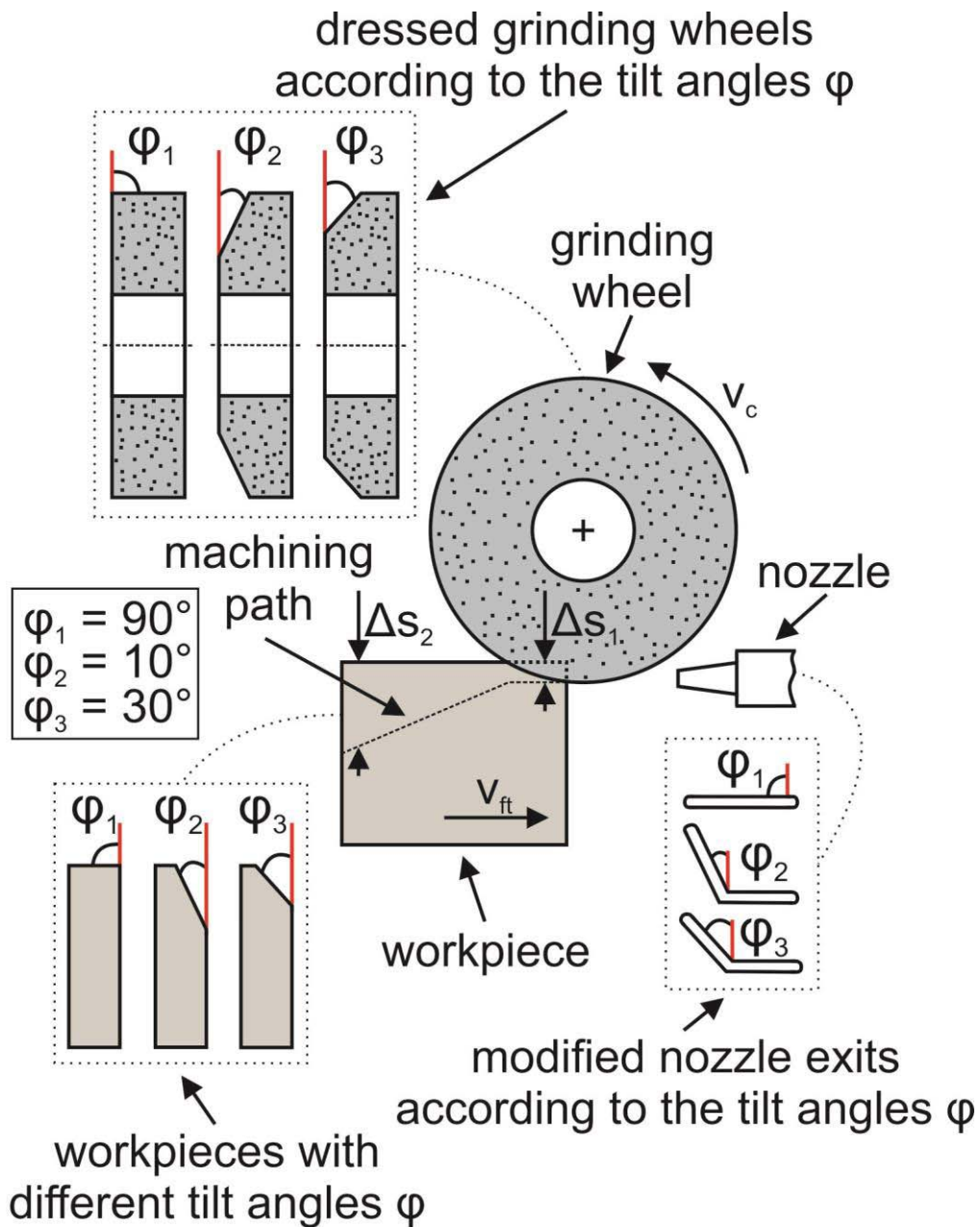


Figure 5. Assignment of the workpieces with different tilt angles to the corresponding points along the involute and the tooth root.

The analogy trials were carried out on the surface grinding machine ELB MicroCut A8 Unicon (Elb-SCHLIFF Werkzeugmaschinen GmbH). The experimental setup used for this purpose is shown schematically in Figure 6.





$\Delta s_1$ : material stock to be removed at the beginning of the grinding process

$\Delta s_2$ : material stock to be removed at the end of the grinding process

Figure 6. Grinding wheel, workpiece and nozzle geometries according to the tilt angle.

Depending on the tilt angles, the grinding wheels were accordingly dressed with a single-point diamond dresser. In order to ensure a comparable fluid supply, the coolant nozzles and the fluid flow rate  $Q_{MWF}$  were adapted. To minimize the experimental effort,

1 grinding experiments with a continuously increasing depth of cut  $a_e$  at a constant tan-  
2 gential feed speed  $v_{ft}$  were carried out whereby the tangential feed speed was in-  
3 creased in 1000 mm/min steps up to 6000 mm/min. At each experiment, the depth of  
4 cut  $a_e$  was increased so that the material stock to be removed  $\Delta s$  was increased from  
5  $\Delta s_1 = 100 \mu\text{m}$  to  $\Delta s_2 = 300 \mu\text{m}$ . The required depths of cut  $a_e$  according to the tilt angles  
6 were calculated using equation 6.  
7  
8  
9

$$10 \quad a_e = \frac{\Delta s}{\sin \varphi} \quad (6)$$

11 Using this procedure a total of 18 experiments were carried out, whereby each test  
12 was performed three times for statistical verification. In order to ensure a uniform ma-  
13 terial removal according to the depth of cut and to compensate the distortion from heat  
14 treatment, the workpieces were also pre-ground. After pre-grinding, the workpieces  
15 were measured geometrically (height H, width W, length L, tilt angle  $\varphi$ ) to ensure a  
16 comparable geometry and thus a common base for the main investigations. The work-  
17 piece dimensions, the process and dressing parameters as well as the grinding wheel  
18 specification and the cooling strategy can be found in Table 2. For the assessment of  
19 the grinding power, the tangential force  $F_t$  was measured using the force plate type  
20 9255B (Kistler Instruments GmbH).  
21  
22  
23  
24  
25  
26  
27  
28  
29  
30  
31  
32  
33  
34  
35  
36  
37  
38  
39  
40  
41  
42  
43  
44  
45  
46  
47  
48  
49  
50  
51  
52  
53  
54  
55  
56  
57  
58  
59  
60  
61  
62  
63  
64  
65



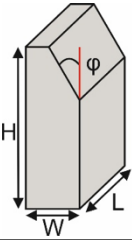
Workpiece			Grinding parameters (Up-Grinding)	
Height	H = 89 mm		Cutting speed	$v_c = 35$ m/s
Width	W = 21 mm	Depth of cut	$a_e = 0.1 - 1.728$ mm	
Length	L = 89 mm	Tilt angle	$\varphi = 10^\circ$	
	$\varphi = 90^\circ$		$\varphi = 30^\circ$	
Grinding wheel		Pre-Grinding parameters (Up-Grinding)		
Specification: 9A60H16VCF2 (white corundum)		Cutting speed	$v_c = 35$ m/s	Depth of cut $a_e = 2 \times 10$ $\mu$ m Tangential feed speed $v_{ft} = 2000$ mm/min
Metal working fluid (MWF) supply		Depth of cut	$a_e = 2 \times 10$ $\mu$ m	
Oil-based (Houghton Cut-Max 902-10)		Dressing conditions		
Conventional tangential nozzle		Dresser: single-point diamond		
	$Q_{MWF, \varphi=90^\circ} = 52$ l/min	Dressing speed	$v_d = 35$ m/s	Dressing depth of cut $a_{de} = 3 \times 10$ $\mu$ m Overlapping ratio $U_d = 3$
Flow rate	$Q_{MWF, \varphi=10^\circ} = 54.1$ l/min	Dressing depth of cut	$a_{de} = 3 \times 10$ $\mu$ m	
	$Q_{MWF, \varphi=30^\circ} = 62.4$ l/min	Overlapping ratio	$U_d = 3$	

Table 2. Summary of the used grinding, pre-grinding and dressing conditions as wells as the workpiece geometry, the grinding wheel specification and the cooling strategy.

The test for a thermal damage (grinding burn) was carried out on the ground gears and on the workpieces by means of nital etching, Barkhausen noise, the preparation of metallographic cross sections and course of hardness beneath the surface. The occurrence of tempering zones in combination with a decrease in hardness was defined as the beginning of thermal impact.

#### 4. Results and discussion

##### *Surface layer modification chart for discontinuous profile grinding of gears*

To generate the surface layer modification chart for discontinuous profile grinding, the calculations of the specific grinding power  $P_c$  and the contact time  $\Delta t$  were carried out using equation 1 and 2. The width of cut  $a_p$  was 13.6 mm and the effective grinding wheel diameter  $d_{s,eff}$  was 215.3 mm (Table 1). In a first approach the conditions (material stock to be removed  $\Delta s$  and contact length  $l_g$  on the pitch circle were assumed for the whole profile, despite it is known that the local material stock to be removed  $\Delta s$  is not constant along the profile. Nevertheless, the distribution of the current grinding

power  $P_c$  in profile direction is not known so that these averaged conditions were assumed. With the specific grinding power and the contact time, as well as the information whether or not grinding burn occurred, it was possible to generate the surface layer modification chart shown in Figure 7. Additionally, two metallographic cross sections are shown to illustrate how thermally influenced gears were distinguished from thermally not influenced gears. The boundary of the tempering zone was determined visually and by means of course of hardness beneath the surface. Furthermore, the course of the thermal limit is qualitatively drawn in the surface layer modification chart up to the contact time of about 0.06 s. From this contact time only a raw guess of the further course of the thermal limit could be made due to missing data points (dotted line), whereby it was ensured that all measuring points at which thermal impact occurred were above this thermal limit.

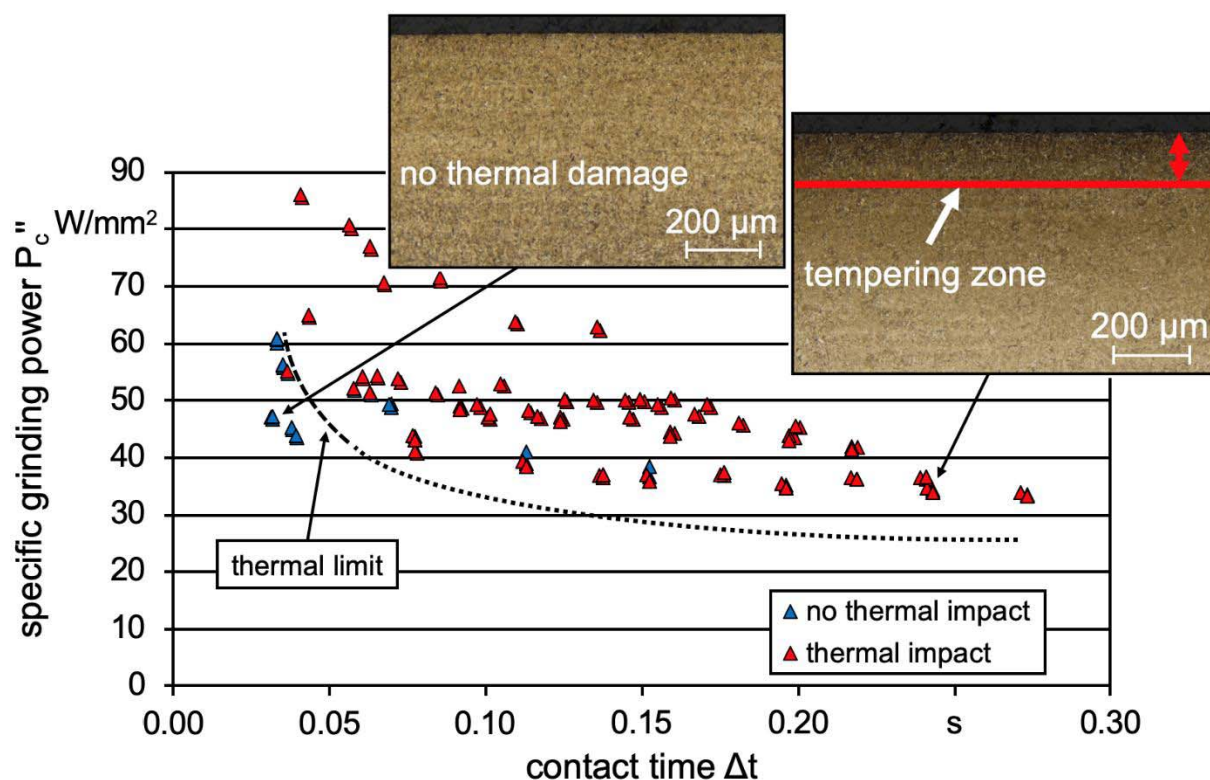


Figure 7. Surface layer modification chart for discontinuous profile grinding of gears.

It can be determined that a thermal impact can occur at all contact times from a certain specific grinding power. In industrial practice, this means that grinding burn cannot be reliably avoided even by choosing small depths of cut and thus short contact times. The fact that some measurement points at which no thermal impact occurred, are

above the thermal limit, could be attributed to measurement uncertainties. It should be noted that this surface layer modification chart only applies to the selected combination of grinding wheel specification, metal working fluid, material and material condition (heat treatment).

### Surface layer modification chart for grinding of workpieces with different tilt angles (analogy trials)

For the generation of the surface layer modification chart based on the results of the analogy trials, it should be noted that different contact conditions existed between the grinding wheel and the workpiece according to the tilt angle  $\phi$  (Figure 8). This has a direct influence on the calculation of the specific grinding power and the contact time.

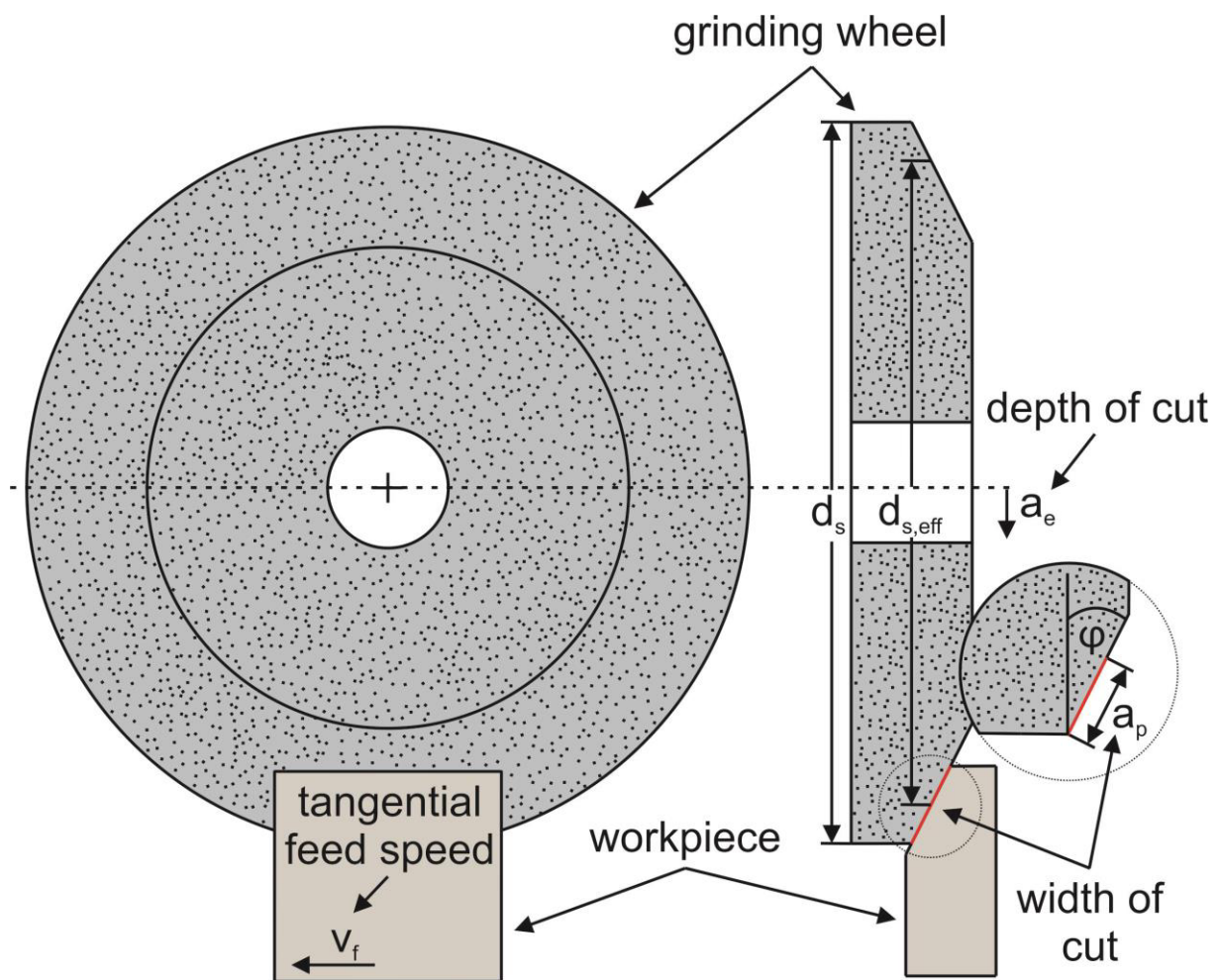


Figure 8. Contact conditions during grinding of workpieces with different tilt angles.

The width of cut  $a_p$  was determined on the respective grinding wheels for all angles. With the help of the width of cut, the effective grinding wheel diameter  $d_{s,eff}$ , which lies in the middle of the contact zone, could be calculated with equation 7.

$$d_{s,eff} = d_s - a_p \cdot \cos \varphi \quad (7)$$

In addition, the cutting speed  $v_c$  was determined as a function of the effective grinding wheel diameter. The values for the width of cut, the effective grinding wheel diameter and the cutting speed are summarized in Table 3.

tilt angle $\varphi$	90°	10°	30°
width of cut $a_p$	21.0 mm	22.5 mm	25.5 mm
grinding wheel diameter $d_s$	380 mm	375 mm	375 mm
effective grinding wheel diameter $d_{s,eff}$	380 mm	356 mm	350 mm
cutting speed $v_c$	35.0 m/s	32.8 m/s	32.2 m/s

Table 3. Measured width of cut and grinding wheel diameter as well as calculated effective grinding wheel diameter and cutting speed according to the tilt angle.

Using the values given in Table 3, it was possible to calculate the contact time according to equation 1 and the specific grinding power with consideration of the measured grinding tangential forces  $F_t$  with equation 8.

$$P_c'' = \frac{F_t(\varphi) \cdot v_c(\varphi)}{a_p(\varphi) \cdot l_g(\varphi)} \quad (8)$$

With the calculated specific grinding power, the corresponding contact times and the information whether or not grinding burn occurred, the surface layer modification chart shown in Figure 9 could be generated. As in the surface layer modification chart for discontinuous profile grinding (Figure 7), the course of the thermal limit was qualitatively inserted from the contact time of about 0.12 s. Until this contact time only a raw guess of the thermal limit could be made due to the missing data points. **The fact that a measurement point at which no thermal impact occurred is above the thermal limit, could be attributed to measurement uncertainties.**

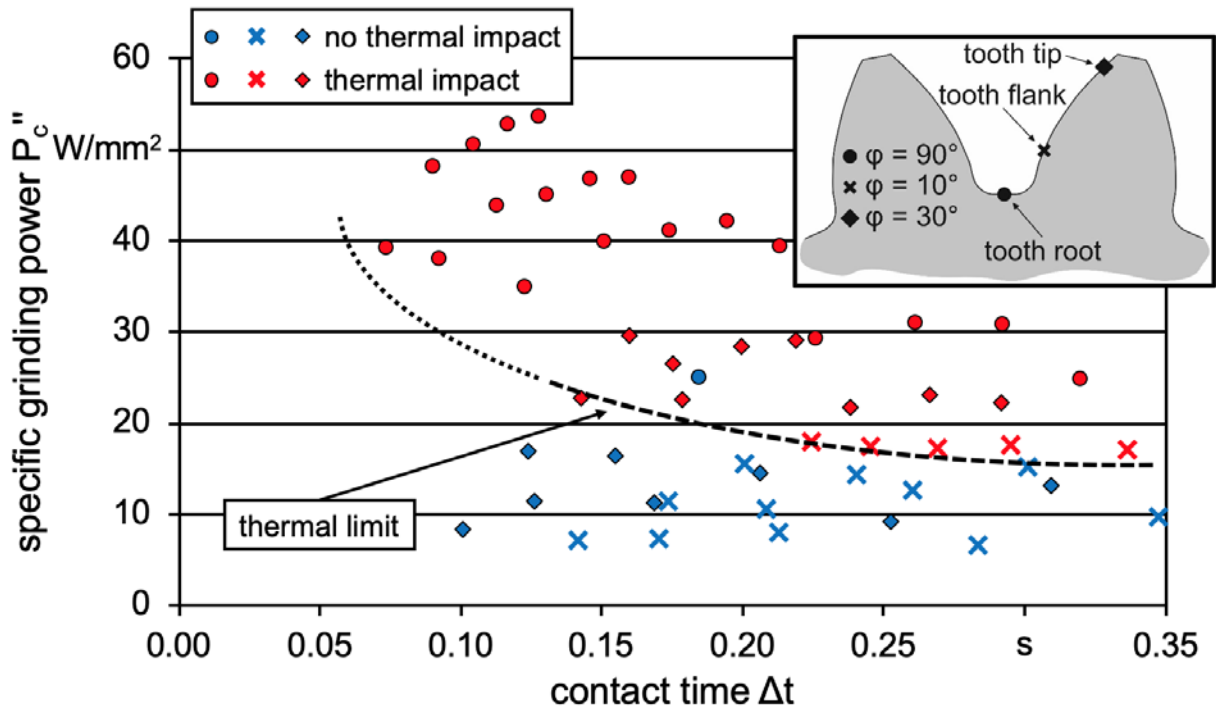


Figure 9. Surface layer modification chart for grinding of workpieces with different tilt angles (analogy trials).

It can be determined that despite identical process parameters (depth of cut and tangential feed speed), the occurrence of grinding burn is significantly influenced by the tilt angle. The risk of thermal damage increases with higher tilt angles. For example, workpieces with the tilt angle of  $10^\circ$  only showed thermal impact in eight cases. In contrast, almost all workpieces with a tilt angle of  $90^\circ$  were thermally influenced. Since the machining conditions for individual areas along the involute and the tooth root are to be investigated with the workpieces with the different tilt angles, this means that grinding burn occurs primarily in the area of the tooth root and on the tooth tip. On the other hand, there is a low risk of thermal damage in the area of the tooth root. This behavior can be explained by the specific tangential forces  $F_t''$  (Figure 10). These were calculated according to equation 9.

$$F_t'' = \frac{F_t(\varphi)}{a_p(\varphi) \cdot l_g(\varphi)} \quad (9)$$

Figure 10 shows the specific tangential forces for a tangential feed speed  $v_{ft}$  of 3000 mm/min.

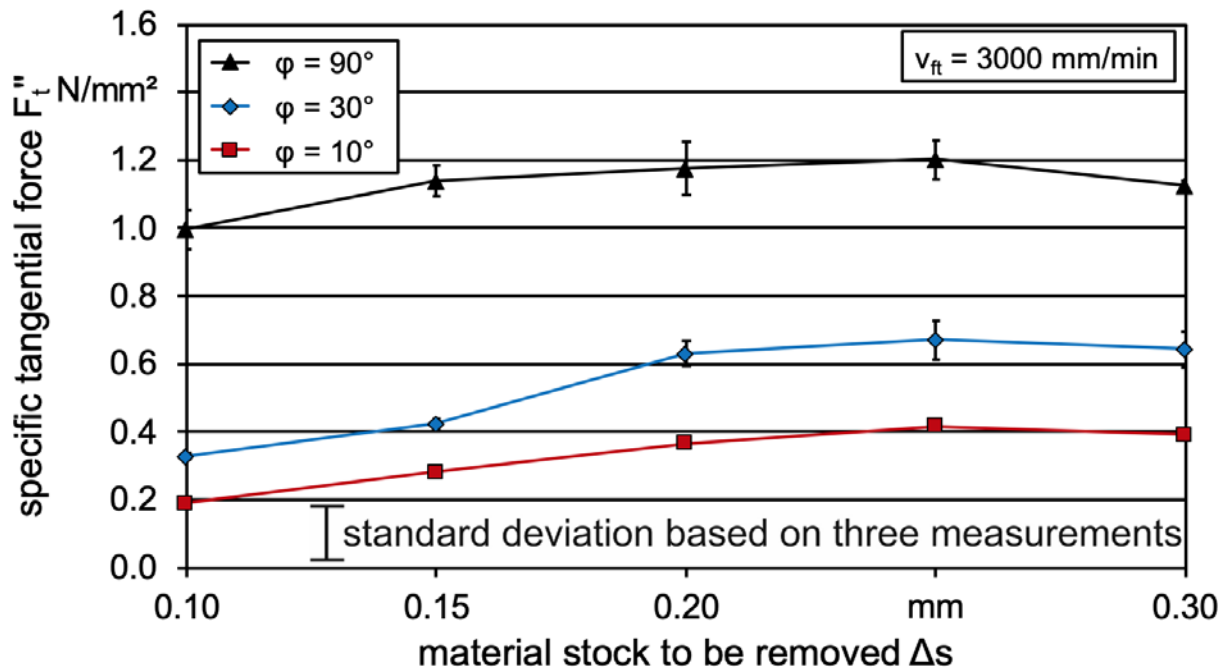


Figure 10. Dependency of the specific tangential force on the tilt angle.

It can be seen that with increasing tilt angle, the specific tangential forces also increase significantly. This in turn means that the workpieces with larger tilt angles are subject to greater thermal load which increases the risk of thermal damage.

### **Combination and comparison of both surface layer modification charts**

In Figure 11, the generated surface layer modification charts for discontinuous profile grinding of gears and grinding of the workpieces with the different tilt angles (analogy trials) are shown in a common diagram. The qualitative courses of the thermal limit were also adopted.



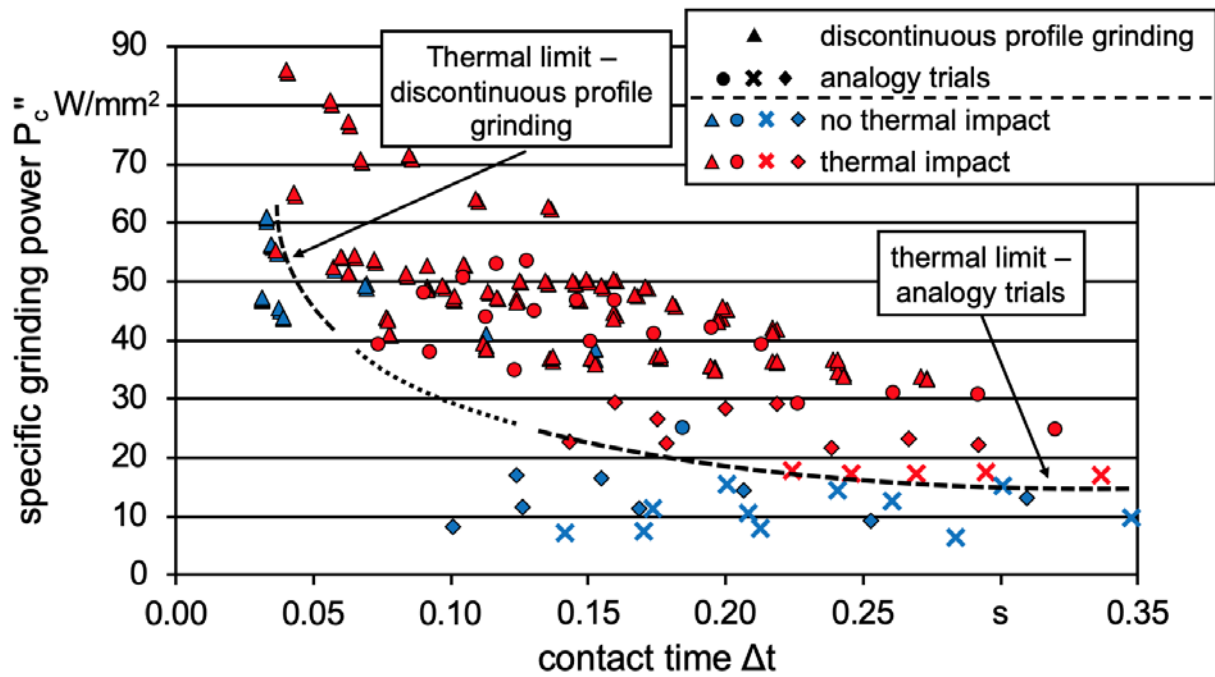


Figure 11. Combination of both surface layer modifications charts.

In general, an overlap of both diagrams can be observed between a specific grinding power  $P_c''$  of 30 W/mm<sup>2</sup> to 60 W/mm<sup>2</sup> and between contact times  $\Delta t$  of 0.07 s and 0.27 s. It can also be determined that the courses of the thermal limit merge into each other, which is indicated by the dotted line. These results suggest that the generation of surface layer modification charts for discontinuous profile grinding can also be done by means of analogy trials. Furthermore, it can be found that the values for the specific grinding power for the analogy trials are lower than the values for discontinuous profile grinding. For the analogy trials the specific grinding power varies between 8 W/mm<sup>2</sup> and 53 W/mm<sup>2</sup> and for discontinuous profile grinding between 33 W/mm<sup>2</sup> and 86 W/mm<sup>2</sup>. Here it can be assumed that this could be mainly due to the lower feed speeds. Feed speeds up to 10000 mm/min were selected for discontinuous profile grinding, whereas up to 6000 mm/min were used for the analogy trials due to the capabilities of the different machine tools used. Further analogy trials with higher feed speeds should therefore be attempted. In these experiments, in addition to the higher feed rates, the material to be removed should be chosen below 100  $\mu\text{m}$  in order to identify the specific grinding power at which grinding burn occurs for contact times between 0.06 s and 0.12 s. With such experiments the dotted line and thus the raw guess of the thermal limit between this contact times could be confirmed.



The overlap of both surface layer modification charts, despite the different system parameters such as grinding wheel specifications, coolants and their supply conditions used in the respective grinding processes, indicates that with the help of the specific grinding power  $P_c''$  not only the influence of the geometry but also influences from other system parameters of the grinding process can be taken into account. Thus the use of such surface layer modification charts ( $P_c''-\Delta t$ ) would certainly depend on the material of the workpieces to be ground and the grinding process, but not necessarily or much less on the system parameters.

In order to check the material dependency, the Malkin data shown in Figure 2 was included in the diagram. His data was determined with different steels, machined with different system parameters, whereby Malkin identified one grinding burn limit for all investigated, hardened, carbon and low-to-medium-alloy steels. Figure 12 shows the experimental points of the gear profile grinding (Figure 7) and analogy trials (Figure 9) in a surface layer modification chart ( $P_c''-\Delta t$ ), the resulting process limits for the case hardened AISI 5120 steel and Malkin's data which led to grinding burn on different hardened steels.

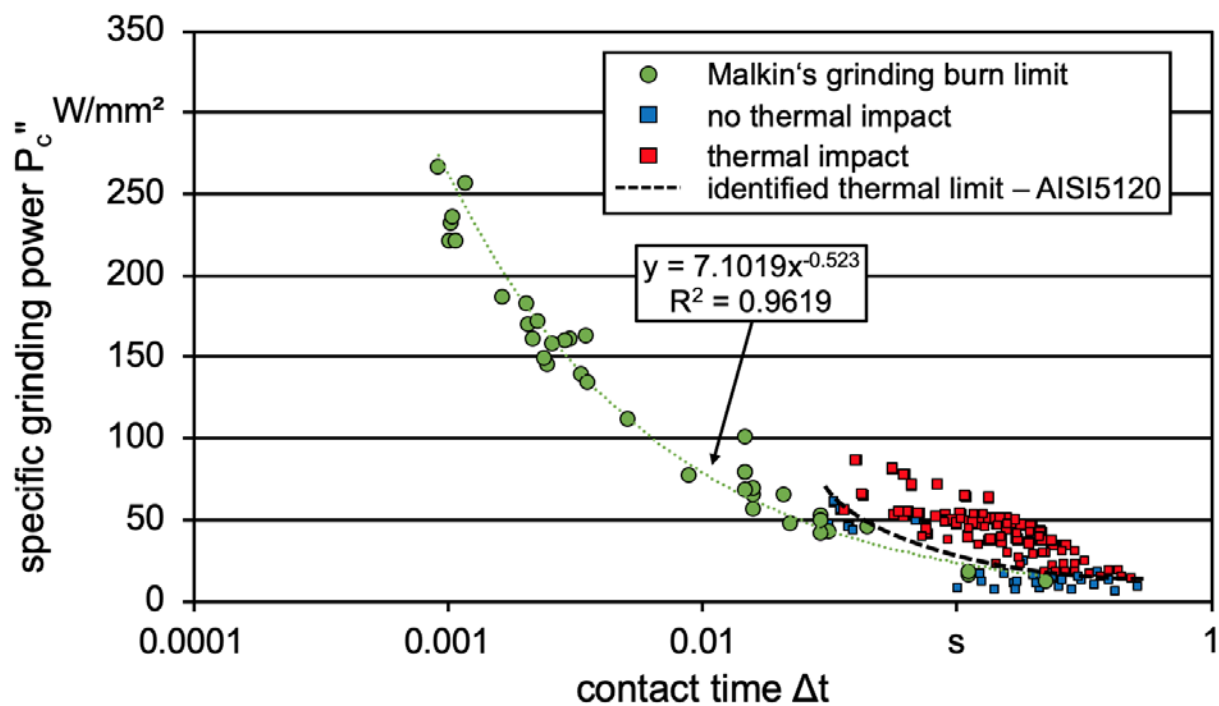


Figure 12. Experimental data of Malkin and the identified thermal process limit in a surface layer modification chart (type 2,  $P_c''-\Delta t$ ).

1  
2  
3  
4  
5  
6  
7  
8  
9  
10  
11  
12  
13  
14  
15  
16  
17  
18  
19  
20  
21  
22  
23  
24  
25  
26  
27  
28  
29  
30  
31  
32  
33  
34  
35  
36  
37  
38  
39  
40  
41  
42  
43  
44  
45  
46  
47  
48  
49  
50  
51  
52  
53  
54  
55  
56  
57  
58  
59  
60  
61  
62  
63  
64  
65

It can be seen that the investigation which was done in this work is very well in line with the grinding results of Malkin. The determined process limits are almost identical. Although different system parameters and different steels which were ground one specific process limit seems to be existent. Due to the fact that even different cooling conditions do not result in a significant shift of the process limit, the question arises as to the differences in heat distribution. The results presented in this work reveal that there is at least a group of steel materials which seems to share a similar thermal process limit, which either indicates similar heat distributions in the different investigations or a much less effect of the heat distribution factor on the burning limits than usually assumed.

## 5. Conclusion and outlook

By means of surface layer modification charts, the occurrence of thermal impact and thus the risk of grinding burn can be detected without additional analysis effort and a quick process adjustment can be carried out, e.g. by adaption the process parameters. The generation of such diagrams for discontinuous profile grinding of gears is time and cost-intensive due to the high demand on gears, the high experimental and the subsequent analysis effort for the detection of grinding burn. With the present work it was shown that surface layer modification charts for discontinuous profile grinding can also be generated by means of analogy trials. For this purpose, surface layer modification charts based on the results after discontinuous profile grinding of gears as well as after grinding of workpieces with different tilt angles were created and then merged. Despite different system parameters in the grinding processes, matching thermal limits were found. The experimental and the analysis effort for the analogy trials prove to be significantly more time and cost saving. In future analogy trials, in which both higher tangential feed speeds and lower material stock to be removed are to be aimed at, the surface layer modification chart shown in Figure 11 is to be completed mainly in the area of contact times between 0.06 s and 0.12 s. This could confirm the course of the dotted line and thus the raw guess of the thermal limit in this area.

The results also suggest that system parameters such as the grinding wheel specification or the cooling strategy are taken into account by the specific grinding power. Thus, the experimental results of this work allow the assumption that the determined process limit is not or just to a low extent depending on the system parameters. This

1 assumption is supported by the thermal process limit determined by Malkin and con-  
2 verted in surface layer modification charts. Malkin's limit, identified for different ground  
3 steels with surface and cylindrical grinding processes and thus different system and  
4 process parameters, corresponds to the results generated in this work at workpieces  
5 ground with a kinematically more complex process. That is the reason why the inves-  
6 tigation of the material dependency of this thermal limit is part of future work. The re-  
7 sults reveal that there is at least a group of steel materials which seems to share a  
8 **similar thermal** process limit. Additionally the application of Malkin's process model for  
9 kinematically more complex grinding processes such as discontinuous profile grinding  
10 should be investigated further in more detail.  
11  
12  
13  
14  
15  
16  
17  
18  
19  
20

## 21 **Acknowledgements**

22 The authors of this paper would like to thank the Deutsche Forschungsgemeinschaft  
23 (DFG) for funding the project HE3276/6-3, which comprised the experimental investi-  
24 gations reported here.  
25  
26

27 Furthermore the scientific work has been supported by the DFG within the research  
28 priority program SPP 2086. The authors thank the DFG for this funding within  
29 KA1006/28-1, which contributed the transfer of the analytical process model to the  
30 complex kinematic of gear profile grinding.  
31  
32  
33  
34  
35  
36  
37  
38

## 39 **References**

- 40 [1] Rowe W B (2018) *Towards High Productivity in Precision Grinding*, MDPI In-  
41 ventions.
- 42 [2] Guo Y B, Warren A W, Hashimoto F (2010) *The basic relationships between*  
43 *residual stress, white layer, and fatigue life of hard turned and ground surfaces*  
44 *in rolling contact*, CIRP Journal of Manufacturing Science and Technology,  
45 Volume 2/2010:129-134.  
46
- 47 [3] Jermolajev S, Epp J, Heinzl C, Brinksmeier E (2016) *Material Modifications*  
48 *Caused by Thermal and Mechanical Load During Grinding*, Procedia CIRP  
49 (45):43– 46.  
50
- 51 [4] Tönshoff H K, Brinksmeier E (1980) *Determination of Mechanical and Thermal*  
52 *Influences on Machined Surfaces by Microhardness and Residual Stress Anal-*  
53 *ysis*, CIRP Annals (29):519-530.  
54
- 55 [5] Brinksmeier E, Klocke F, Lucca D A, Sölter J, Meyer D (2014) *Process Signa-*  
56 *tures – a new approach to solve the inverse surface integrity problem in ma-*  
57 *chining processes*, Procedia CIRP (13):429-434.  
58  
59  
60  
61  
62  
63  
64  
65

- 1  
2  
3  
4  
5  
6  
7  
8  
9  
10  
11  
12  
13  
14  
15  
16  
17  
18  
19  
20  
21  
22  
23  
24  
25  
26  
27  
28  
29  
30  
31  
32  
33  
34  
35  
36  
37  
38  
39  
40  
41  
42  
43  
44  
45  
46  
47  
48  
49  
50  
51  
52  
53  
54  
55  
56  
57  
58  
59  
60  
61  
62  
63  
64  
65
- [6] Field M, Koster W (1978) *Optimizing grinding parameters to combine high productivity with high surface integrity*, CIRP Annals (27/1):523-526.
  - [7] Jaeger J C (1942) *Moving Sources of Heat and the Temperature at Sliding Contacts*, Proceedings of the Royal Society of New South Wales (76):203-224.
  - [8] Carslaw H S, Jaeger J C (1959) *Conduction of Heat in Solids*, Oxford University Press.
  - [9] Des Ruisseaux N R (1968) *Thermal Aspects of Grinding Processes*, PhD thesis, University of Cincinnati.
  - [10] Malkin S (1978) *Burning Limit for Surface and Cylindrical Grinding of Steels*, CIRP Annals (27):233–236.
  - [11] Heinzl C (2009) *Schleifprozesse verstehen: Zum Stand der Modellbildung und Simulation sowie unterstützender experimenteller Methoden*, post-doctoral thesis, University of Bremen.
  - [12] Malkin S, Guo C (2007) *Thermal Analysis of Grinding*, CIRP Annals (56/2):760–782.
  - [13] Heinzl C, Sölter J, Jermolajev S, Kolkwitz B, Brinksmeier E (2014) *A versatile method to determine thermal limits in grinding*, Procedia CIRP (13):131-136.
  - [14] Karpuschewski B, Knoche H J, Hipke M (2008) *Gear Finishing by Abrasive Processes*, CIRP Annals (57/2):621–640.
  - [15] Fradkin E (2003) *Precision of the Large-Module Ground Gears From Different Steels (in Russian)*, Vestnik Masinstroenija (4):58–63.
  - [16] Jawahir I S, Brinksmeier E, M'Saoubi R, Aspinwall D K, Outeiro J C, Meyer D, Umbrello D, Jayal A D (2011) *Surface Integrity in material removal processes: Recent advances*, CIRP Annals – Manufacturing Technology, Volume 60/2:603-626.
  - [17] Meyer L W (2006) *Einsatz von Temperatur- und Kraftsensoren in Schleifwerkzeugen*, PhD thesis, University of Bremen.
  - [18] Meyer D, Wagner A (2016) *Influence of metalworking fluid additives on the thermal conditions in grinding*, CIRP Annals (65):313-316.
  - [19] Jermolajev S, Brinksmeier E (2014) *A new approach for the prediction of surface and subsurface properties after grinding*, Advanced Materials Research (1018):189-196.
  - [20] Fricker D, Pearce T, Harrison A (2004) *Predicting the occurrence of grind hardening in cubic boron nitride grinding of crankshaft steel*, Proceedings of the Institution of Mechanical Engineers, Part B: Journal of Engineering Manufacture:1339-1356.
  - [21] Foeckerer T, Kolkwitz B, Heinzl C, Zaeh M F (2012) *Experimental and numerical analysis of transient behavior during grind-hardening of AISI 52100*, In: Production Engineering - Research and Development (6/5):559-568.
  - [22] Kolkwitz B, Foeckerer T, Heinzl C, Zaeh M F, Brinksmeier E (2011) *Experimental and Numerical Analysis of the Surface Integrity resulting from Outer-Diameter Grind- Hardening*, Procedia Engineering (19):222-227.

- 1  
2  
3  
4  
5  
6  
7  
8  
9  
10  
11  
12  
13  
14  
15  
16  
17  
18  
19  
20  
21  
22  
23  
24  
25  
26  
27  
28  
29  
30  
31  
32  
33  
34  
35  
36  
37  
38  
39  
40  
41  
42  
43  
44  
45  
46  
47  
48  
49  
50  
51  
52  
53  
54  
55  
56  
57  
58  
59  
60  
61  
62  
63  
64  
65
- [23] Jermolajev S, Heinzl C, Brinksmeier E (2015) *Experimental and Analytical Investigation of Workpiece Thermal Load During External Cylindrical Grinding*, Procedia CIRP (31):465-470.
  - [24] Jermolajev S, Brinksmeier E, Heinzl C (2018) *Surface layer modification charts for gear grinding*, CIRP Annals (67):333-336.
  - [25] Brinksmeier E, Eckebrecht J, Wilkens A (2011) *Wheel Based Temperature Measurement in Grinding*, Advanced Materials Research (325):3-11.
  - [26] Minke E, Heinzl C (2000) *Werkstückrandzonenausbildung in der schleifenden Bearbeitung*. In: Schleiftechnik im Wettbewerb – Stand der Technik und Zukunftschancen des Fertigungsverfahrens. Hrsg. W. Wicharz, F. Klocke, E. Brinksmeier, Bremen, Selbstverlag:15-1.
  - [27] Brockhoff T (1999) *Schleifprozesse zur martensitischen Randschichthärtung von Stählen*, PhD thesis, University of Bremen.
  - [28] Wilke T (2008) *Energieumsetzung und Gefügebeeinflussung beim Schleifhärten*, PhD thesis, University of Bremen.
  - [29] Stephenson D J, Jin T (2003) *Physical Basics in Grinding*, European Conference on Grinding, Aachen.
  - [30] Jin T, Stephenson D J (2003) *Investigation of the heat partitioning in high efficiency deep grinding*, International Journal of Machine Tools & Manufacture (43):1129-1134.
  - [31] Jin T, Stephenson D J (2006) *Analysis of grinding chip temperature and energy partitioning in high-efficiency deep grinding*, Proc. IMechE Vol. 220 Part B: J. Engineering Manufacture.
  - [32] Lavine A S (1988) *A Simple Model for Convective Cooling During the Grinding Process*, Journal of Engineering for Industry (110/1):1-6.
  - [33] Rowe W B, Pettit J A, Boyle A, Moruzzi J L (1988) *Avoidance of Thermal Damage in Grinding and Prediction of the Damage Threshold*, CIRP Annals (37/1):327-330.
  - [34] Voll M (2001) *Modelle zur thermischen Optimierung von Trockenschleifprozessen*, PhD thesis, University of Zwickau.
  - [35] Schlattmeier H (2004) *Diskontinuierliches Zahnflankenprofilschleifen mit Korund*, PhD thesis, RWTH Aachen.